



Injectable CNPs/DMP1-loaded self-assembly hydrogel regulating inflammation of dental pulp stem cells for dentin regeneration

Yue Zhao^{a,b,1}, Lutong Song^{a,b,1}, Mengchen Li^{a,b}, Haoran Peng^{a,b}, Xinyi Qiu^{a,b}, Yuyang Li^{a,b}, Bijun Zhu^{a,b}, Chao Liu^{b,c,***}, Shuangshuang Ren^{a,b,**}, Leiying Miao^{a,b,*}

^a Department of Cariology and Endodontics, Nanjing Stomatological Hospital, Affiliated Hospital of Medical School, Nanjing University, Nanjing, China

^b Central Laboratory of Stomatology, Nanjing Stomatological Hospital, Affiliated Hospital of Medical School, Nanjing University, Nanjing, China

^c Department of Orthodontics, Nanjing Stomatological Hospital, Affiliated Hospital of Medical School, Nanjing University, Nanjing, China

ARTICLE INFO

Keywords:

Pulp-capping material
Self-assembly hydrogel
Cerium oxide nanoparticles
Dentin matrix protein-1
Dental pulp stem cells

ABSTRACT

Vital pulp preservation, which is a clinical challenge of aseptic or iatrogenic accidental exposure of the pulp, in cases direct pulp capping is the main technology. Human dental pulp stem cells (hDPSCs) play a critical role in pulp tissue repair, but their differentiative ability could be inhibited by the potential infection and inflammatory response of the exposed pulp. Therefore, inflammatory regulation and differentiated promotion of hDPSCs are both essential for preserving living pulp teeth. In this study, we constructed a functional dental pulp-capping hydrogel by loading cerium oxide nanoparticles (CNPs) and dentin matrix protein-1 (DMP1) into an injectable Fmoc-triphenylalanine hydrogel (Fmoc-phe3 hydrogel) as CNPs/DMP1/Hydrogel for in situ drugs delivery. With a view to long-term storage and release of CNPs (anti-inflammatory and antioxidant) to regulate the local inflammatory environment and DMP1 to promote the regeneration of dentin. Results of CCK-8, LDH release, hemolysis, and Live/Dead assessment of cells demonstrated the good biocompatibility of CNPs/DMP1/Hydrogel. The levels of alkaline phosphatase activity, quantification of the mineralized nodules, expressions of osteogenic genes and proteins demonstrated CNPs/DMP1/Hydrogel could protect the activity of hDPSCs' osteogenic/dentinogenic differentiation by reducing the inflammation response via releasing CNPs. The therapy effects were further confirmed in rat models, CNPs/DMP1/Hydrogel reduced the necrosis rate of damaged pulp and promoted injured pulp repair and reparative dentin formation with preserved vital pulps. In summary, the CNPs/DMP1/Hydrogel composite is an up-and-coming pulp-capping material candidate to induce reparative dentin formation, as well as provide a theoretical and experimental basis for developing pulp-capping materials.

1. Introduction

As is well known, vital pulp provides nutrition for the development of natural teeth, and dentin regeneration is essential for vital pulp preservation therapy (VPT). VPT avoids damage to the pulp-dentin complex and helps protect the remaining pulp tissue, promoting the continued development and closure of the apical foramen in young permanent teeth [1]. Studies have shown that the use of root canal

treatment to remove the vital pulp tissue will make the root canal wall of permanent teeth thin, these fragile molars are easy to fracture over time, seriously affecting the survival rate of teeth [2]. Thus VPT [3], as a treatment approach aimed at preserving vital pulp, has gain more and more attention over the last 20 years [4]. Clinically, the traumatic dental injuries and caries management might expose the pulp and cause aseptic inflammation [5]. There is evidence that lower levels of pro-inflammatory mediators may promote tissue repair [6], while

* Corresponding author. Department of Cariology and Endodontics, Nanjing Stomatological Hospital, Affiliated Hospital of Medical School, Nanjing University, Nanjing, China.

** Corresponding author. Department of Cariology and Endodontics, Nanjing Stomatological Hospital, Affiliated Hospital of Medical School, Nanjing University, Nanjing, China.

*** Corresponding author. Central Laboratory of Stomatology, Nanjing Stomatological Hospital, Affiliated Hospital of Medical School, Nanjing University, Nanjing, China.

E-mail addresses: dxliuchao@163.com (C. Liu), zjndrenss@163.com (S. Ren), miaoleiying80@163.com (L. Miao).

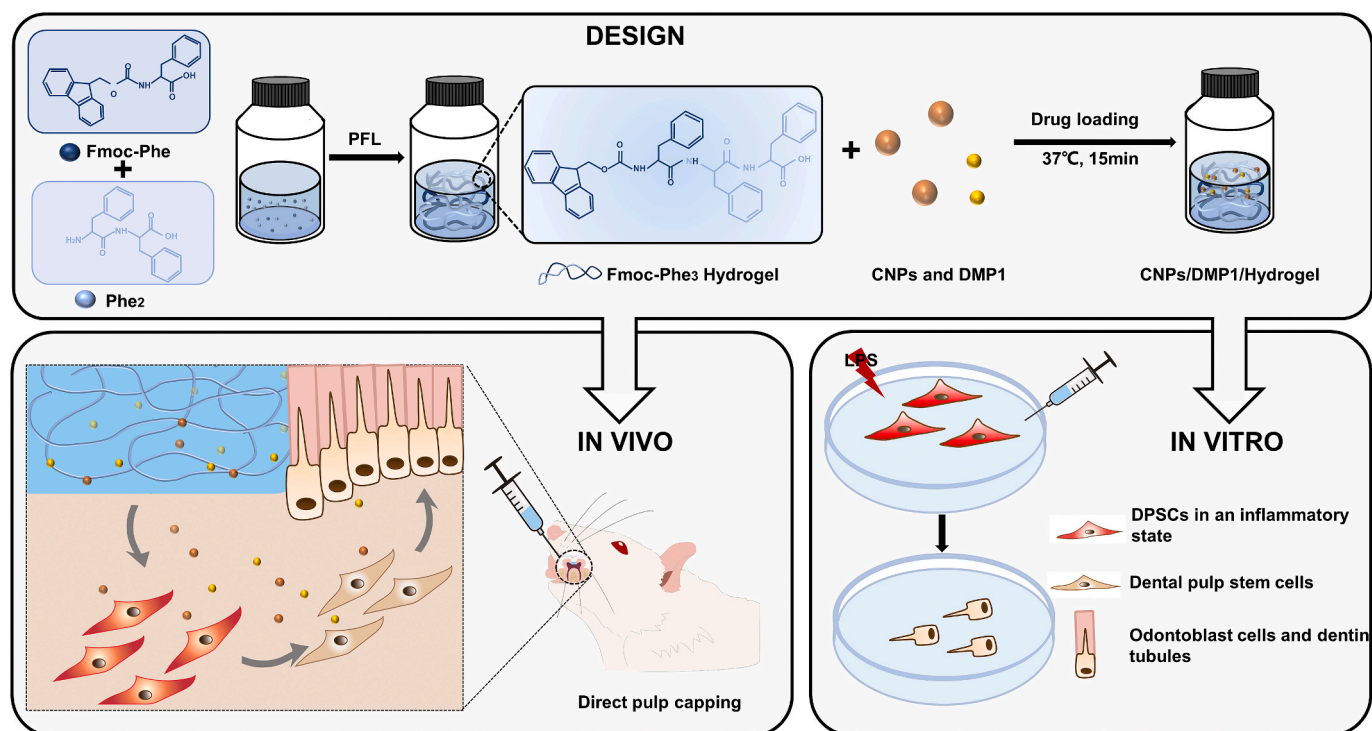
¹ These authors contributed to this work equally.

intense inflammatory could inhibit the differentiative ability of hDPSCs [7,8]. In addition, the pathological process of pulpitis reflects the characteristics of oxidative stress. Inflammatory cells such as neutrophils in pulp tissue engulf harmful substances such as microorganisms and produce a large number of reactive oxygen species (ROS) [9]. The differentiation ability of hDPSCs is closely related to dentin regeneration, and when inflammation persists in the pulp for a long time, the level of ROS increases, and the differentiation ability of pulp stem cells decreases. In short, if the inflammation persists in the pulp tissue, it will hinder the regeneration process of the pulp tissue and eventually lead to pulp necrosis [10] (see Scheme 1).

Therefore, controlling inflammation is essential to protect the differentiation ability of hDPSCs. In clinical practice, pulp capping agents are often used to avoid dental pulp necrosis and promote the differentiation of hDPSCs into odontoblast cells to promote dentin regeneration [11–13], and these treatments focus on removing the inflammatory pulp and promoting the reparative dentin formation from the remaining normal stem cells. Currently, the clinic's commonly used pulp capping agents include calcium hydroxide cements (CHC), mineral trioxide aggregate (MTA), and iRoot BP Plus [14]. CHC may lead to irreversible inflammation and pathological pulp calcification [15]. Compared with CHC, MTA cements have a higher success rate [16], with a lower inflammatory response and a more predictable hard dentin barrier formation [17]. However, MTA could increase the ROS levels in hDPSCs [17]. The iRoot BP Plus has a slightly shorter clotting time, but is expensive and exhibits higher cytotoxicity than MTA and could lead to mild to moderate inflammation in the pulp tissue [18,19]. Therefore, developing new agents with the ability of anti-inflammatory, protect pulp stem cells and rapidly mobilize hDPSCs to promote the repairment of damaged pulp tissue, is still essential [20]. With the development of the material field, researchers have found that many biological materials can inhibit pulpitis and enhance the differentiation ability of hDPSCs, Such as baicalensis [21] and Curcumin [22] isolated from medicinal plant. In addition to this, many nanomaterials have also shown excellent anti-inflammatory ability, such as folic acid modified silver nanoparticles (FA-AgNPs) and [23]gold nanoparticles (AuNPs) [24]. Cerium

oxide nanoparticles (CNPs) are stable lanthanide metal element oxide with low cost, it had been reported to have superoxide dismutase (SOD)-like activity and exert anti-inflammatory and antioxidant functions [25,26]. In oral-related diseases, CNPs have been found to treat *peri-implantitis* and *periodontitis* [27,28]. In studies on hDPSCs, CNPs mixed with MTA effectively reduced the high ROS levels produced by MTA [29,30]. Our previous study revealed the differentiation ability of human periodontal stem cells (hPDLSCs) could be decreased under continuous LPS exposure for oxidative stress and inflammation micro-environment simulation, which could be recovered by the pretreatment of CNPs [31]. For the anti-inflammatory ability, CNPs might potentially control pulpitis to create a regenerative environment, as an ideal strategy for dentin regeneration. However, the effect of CNPs on the differentiation ability of hDPSCs in an intense inflammatory environment has not been investigated yet. Growth proteins have received much attention among the studies that promote dentinogenic differentiation of pulp stem cells. DMP1 is a highly phosphorylated acidic non-collagenous protein in dentin and bone, with promising applications [32,33]. DMP1 has many acidic structural domains, carries a negative charge, and has a strong binding capacity to calcium ions, which promote hydroxyapatite formation and participate in the mineralization process of hard tissues *in vivo*. It is vital in regulating bone mineralization and inducing differentiation of bone marrow mesenchymal stem cells and dental pulp stem cells [34–36].

However, the disadvantage is that CNPs and DMP1 can only be injected locally, as a limitation in further clinical application. Controlled drug delivery systems for bioactive agents [37] for dentin regeneration could be promising. Hydrogels are polymer materials with three-dimensional network structures, one of the main advantages of hydrogels is that they can be used as a drug delivery system for various bioactive agents, thus endowing hydrogels with various effective functions. Hydrogels can be synthetic or natural. Polypeptide hydrogels, a subgroup of natural hydrogels, have many advantages in the field of biological drug delivery [38]. Polypeptide hydrogels compared with calcium-based pulp capping materials such as MTA, Fmoc-phe3 hydrogel is a biocompatible carrier, which can not only load various



Scheme 1. Schematic illustration of CNPs/DMP1/Hydrogel for dentin regeneration.

anti-inflammatory and pro-differentiation components but also promote the adhesion and proliferation of microglia cells [39]. The possibility of effectively coupling drug delivery systems to hydrogel materials seems particularly promising for tissue engineering applications, where hydrogels can provide cells with the support they need to grow, and nanoparticles can promote cell growth or differentiation by providing cells with the necessary bioactive molecules.

For the localized application of these drugs into tooth cavities, we used an injectable hydrogel, which allows for the incorporation of DMP1 and CNPs. Once placed in the tooth defect, the liquid solidifies upon the action of the Lipase from *Pseudomonas fluorescens* (PFL). Previous studies have reported that Fmoc-phe3 Hydrogel functions as a hydrogel 3D scaffold material [40]. Our research group successfully loaded CNPs into the hydrogel [41]. The objective of this study was to examine the potential anti-inflammatory properties and ability to induce reparative dentin formation of the combination of DMP1 and CNPs. As a result, further investigation into the optimal ratio of CNPs to Fmoc-phe3 is recommended in order to enhance its potential as a novel capping material. The physicochemical characteristics of CNPs and DMP1, when combined with the Fmoc-phe3 hydrogel, were analyzed, and it was demonstrated that the CNPs/DMP1/Hydrogel composite effectively mitigates inflammation and promotes the formation of reparative dentin.

2. Materials and methods

2.1. Materials

Fmoc-Phe and Phe₂ were purchased from Yuanye Biotechnology. Na(OH)₂, HCl, ethylene glycol and Lipase from *Pseudomonas fluorescens* (PFL) were purchased from Aladdin Industrial Corporation. Human DMP1 was purchased from Sino Biological Inc. Ce(NO₃)₃·6H₂O and NH₄OH were purchased from Sigma. All other reagents were of reagent grade.

2.2. Synthesis of CNPs and CNPs/DMP1/hydrogel

The CNPs and Fmoc-phe3 were synthesized following a previously published protocol. A solution of cerium nitrate hexahydrate (Ce(NO₃)₃·6H₂O) with a concentration of 6 mmol was prepared by dissolving it in a mixture of 100 mL of deionized water (ddH₂O) and ethylene glycol in a 1:1 ratio at room temperature. The resulting cerium nitrate solution was then heated to 60 °C, and 20 mL of ammonium hydroxide (NH₄OH) was added. After vigorous stirring for 3 h, cerium nanoparticles (CNPs) were obtained. All the samples were collected and stored in EP tubes at a temperature of 4 °C for subsequent experiments. The effective concentrations of DMP1 and CNPs were determined by conducting a comprehensive literature review and conducting preliminary experiments. Subsequently, the quantities of DMP1 and CNPs required for the synthesis of composite hydrogels were calculated based on the drug loading rate of said hydrogels. Ultimately, the concentrations of DMP1 and CNPs in the composite hydrogel were confirmed to be 1 µg/ml and 80 µg/ml, respectively. In brief, Fmoc-Phe (48 mg) and Phe₂ (36 mg) were accurately weighed and placed on a sterile UV-irradiated surface for a duration of 4 h. PFL (50 mg) was dissolved in 1 mL of deionized water and subsequently filtered through a 0.22 µm filter (Millipore, America). Fmoc-Phe and Phe₂ were dissolved in a mixture of 3 mL PBS (Servicebio, China) and 0.5 M NaOH (1.2 mL). The pH was adjusted to 7.0 using 0.1 M HCl (0.4 mL). Finally, 600 µL of PFL solution was added and incubated at a constant temperature of 37 °C for 15 min. Different samples were prepared by introducing CNPs (80 µg/mL) and DMP1 (1 µg/mL) to the precursor solution.

2.3. Characterization of CNPs and CNPs/DMP1/hydrogel

The size and distribution of cerium nanoparticles (CNPs) were

examined using transmission electron microscopy (TEM, Tecnai G2 Spirit Biotwin, FEI Company, USA) at an acceleration voltage of 15 kV. The presence of CNPs and DMP1 in Fmoc-phe3 hydrogel was observed through scanning electron microscopy (SEM, JSM-6700 F, JEOL, Japan). The zeta-potential value was determined using a Zetasizer instrument (Nano ZS90, Malvern, UK). Fourier transformed infrared (FTIR) analysis was conducted on the Fmoc-phe3 hydrogel and its precursor solution. To obtain the corresponding IR spectra, the hydrogel and hydrogel precursor aqueous solution were dried and analyzed using Thermo Scientific Nicolet iS50 FT-IR spectrometer (Thermo Scientific, Waltham, MA, USA).

In brief, the CNPs/DMP1/Hydrogel, with a reduced amount of PBS, underwent incubation at a temperature of 37 °C in a water bath, which was covered with aluminum foil. The weight change ratio was determined by measuring the loss in weight within the PBS solution. Subsequently, the CNPs/DMP1/Hydrogel underwent freeze-drying and were weighed (W₀), followed by immersion in centrifuge tubes containing 5 mL of PBS. These samples were then incubated in a water bath at a temperature of 37.0 ± 0.4 °C. The weight of each sample after freeze-drying was recorded at the designated time (W_t).

The precipitate of CNPs/DMP1/Hydrogel was collected by centrifugation, and the precipitate was washed three times with PBS to collect the unloaded CNPs and DMP1 solutions. The drug loading efficiency (DLC) was calculated by detecting the drug content in the solutions. In addition, the supernatant was collected at each predetermined time point, the concentration of CNPs or DMP1 in the hydrogel was detected, and the collection solution was supplemented with equal amounts of PBS to calculate the change in drug content. At the end of the experiment, DMP1 was thawed using a Human DMP1 ELISA Kit (Sigma-Aldrich, USA), and CNPs was determined by an ICP spectrometer (Avio 500, PerkinElmer, USA).

2.4. hDPSCs culture

With the Ethics Committee of the Nanjing Stomatological Hospital (contract awarded to NJSH-2022NL-008, Nanjing, China) and the consent of the patients, we collected reduced teeth extracted for orthodontic reasons from 5 healthy individuals (18 years of age). The pulp tissue was extracted from the teeth under aseptic conditions, then cut into 1 × 1 mm² mass and digested with 2 mg/mL collagenase type I (Biofrox, China) for 30 min at 37 °C. After centrifuged and resuspended, The cell pellet was transferred to a 25 mm² tissue culture flask, incubated with DMEM (Gibco, USA) containing 10 % fetal bovine serum (Sigma, USA), 100 U/mL penicillin and 100 U/mL streptomycin (HyClone, USA) at 5 % CO₂ with 37 °C. The hDPSCs between passages 3–5 were used for subsequent experiments.

2.5. In-vitro cytotoxicity analysis

hDPSCs were cultured and selected according to the methodology outlined in our previous study [42]. All experiments were conducted in triplicate. To assess the cytotoxic impact of inflammatory microenvironments and CNPs/DMP1/Hydrogel on cells, a 96-well plate (Corning, USA) was utilized, and cells were seeded at a density of 3.0 × 10³ cells/well for a duration of 24 h. Subsequently, the complete medium conditions were replaced with LPS (0, 0.1, 1, 5, 10, or 20 µg/mL) or various hydrogel treatments (Fmoc-phe3 hydrogel, CNPs/Hydrogel, DMP1/Hydrogel, CNPs/DMP1/Hydrogel). After an incubation period of 1, 3, 5, and 7 days, the cells underwent two washes with PBS. Subsequently, a medium devoid of FBS but containing 10 % of CCK-8 solution (Beyotime Biotechnology, China) was introduced into each well for a 2-h treatment at 37 °C. The absorbance at 450 nm OD values was measured using a SpectraMax M3 enzyme marker (Molecular Devices, CA, USA).

For hemolysis determination, the Sprague-Dawley rats' red blood cells were isolated and diluted with 0.9 % NaCl solution to obtain a 2 % erythrocyte solution. The ddH₂O was used as a positive control and 0.9

% NaCl solution containing different Hydrogel groups were used as experimental samples ($n = 5$). After a total co-incubation time of 24 h at 37 °C, the absorbance at 545 nm OD values was examined using a SpectraMax M3 enzyme marker.

The Live/Dead assessment of cells was also carried out. Cells were seeded in a 6-well plate (Corning, USA) at a density of 1.0×10^5 cells/well and incubated with different hydrogel samples. The cells were washed with PBS and stained with Calcein-AM/Propidium Iodide (CAM/PI) (Dojindo, Japan). Fluorescence photographs were collected using a confocal fluorescence microscope (A1, Nikon, Japan). The counts of the live cells were quantified by the ImageJ software. Cells' fragments and clumps were excluded.

2.6. TEM examination of cells

Cells were initially seeded in a 6-well plate at a density of 1.0×10^5 cells per well and allowed to grow overnight. Subsequently, the cells were incubated with CNPs/DMP1/Hydrogel for a duration of 24 h. Following the treatment, the cells were washed thrice with PBS (KeyGen bioTECH, China) and fixed in 2.5 % glutaraldehyde (Merck, Germany). To immobilize the cells, they were treated with 1 % osmium tetroxide (Merck, Germany) for a period of 2 h and then dehydrated using a gradient of ethanol (Merck, Germany) concentrations: 50 %, 75 %, 95 %, and 100 % for 10 minutes each. Finally, the cells were embedded in epoxy resin for the purpose of obtaining ultrathin sections. These sections were subsequently utilized for TEM (JEM-1011, JEOL) imaging at an acceleration voltage of 120 kV accelerated voltage.

2.7. In vitro anti-oxidative studies

To investigate the ROS scavenging activity of CNPs/DMP1/Hydrogel, the cells were co-cultured with CNPs/DMP1/Hydrogel and LPS (10 $\mu\text{g}/\text{mL}$, Sigma, USA). In brief, hDPSCs were seeded in a 6-well plate with a density of 1.0×10^5 cells/well. When cells reached 60 %, CNPs/DMP1/Hydrogel were added into the medium and cultured for 24 h, then the LPS was added to the medium at concentrations of 10 $\mu\text{g}/\text{mL}$ for 24 h, then washed three with PBS and incubated with a 10 μM DCFH-DA probe (Beyotime Biotechnology, China) for 15 min. The green fluorescence was observed at 488 nm under a confocal fluorescence microscope (Nikon Ti, Japan).

2.8. Real-time quantitative PCR

To investigate the hDPSCs inflammation and differentiation-related gene expression in inflammatory microenvironments, cells were treated with LPS (10 $\mu\text{g}/\text{mL}$) in osteogenic medium (OM, DMEM supplemented with 10 % FBS, 10 mM sodium β - glycerophosphate, 50 mg/mL ascorbic acid, 0.1 μM dexamethasone) for 7 days. Change the medium every 2 days, and LPS is not added when we replace the new medium. Subsequently, an examination was conducted on the expression of genes associated with inflammation and differentiation, namely IL-1 β , IL-6, Interleukin 8 (IL-8), ALP, Runt-related transcription factor 2

(RUNX2), osteocalcin (OCN), DSPP, DMP1, and Bone sialoprotein (BSP). The specific primer sequences can be found in Table 1. Total cellular RNA was isolated using TRIzol (Invitrogen, Karlsruhe, Germany) and quantified using a Thermo Scientific NanoDropt 1000 ultraviolet-visible spectrophotometer (NanoDrop Technologies, Wilmington, DE). Subsequently, the RNA was reverse transcribed into cDNA using the Prime-Script™ II 1st Strand cDNA Synthesis Kit. Each reaction was conducted with a final volume of 10 μL , consisting of 4 μL cDNA, 0.5 mM of each primer, and 5 μL SYBR Green PCR Master Mix (Vazyme Biotech Co, China). The comparative 2- $\Delta\Delta\text{Ct}$ method, utilizing StepOne Software version 2.1.22, was employed to calculate the relative expression levels of the target genes. All samples were subjected to triplicate runs and normalized to GAPDH.

2.9. Osteogenic/dentinogenic differentiation

To induce osteogenic/dentinogenic differentiation in cells, the culture medium was replaced with osteogenic medium (OM) every 3 days. The cells were then cultured in OM medium for 7 and 14 days, and the osteogenic/dentinogenic potential was evaluated using ALP activity assay and NBT/BCIP ALP staining kits (Beyotime Biotechnology, China). For ARS staining, cells were stained with a 10 % ARS solution (Cyagen Biosciences Inc, China) for 14 and 21 days, washed with dd H₂O, and mineral deposition was quantified using a 10 % (w/v) cetylpyridinium chloride solution (Sigma-Aldrich), and the staining intensity was quantified by measuring the absorbance at 562 nm in a microplate reader (Bio-Tek). All experiments were conducted in triplicate.

2.10. Western blotting

Total cellular protein was extracted from cultured cell populations using the RIPA buffer (Thermo Scientific, USA) supplemented with a protease inhibitor cocktail (Keygen Biotechnology, China), following the manufacturer's instructions. The protein concentration was determined using the BCA Protein Assay Kit (Beyotime, China). Protein samples were loaded at a concentration of 10 μg per well on a 10 % dodecyl sulfate (SDS)-polyacrylamide gel electrophoresis (10 %, 15 wells, GenScript, China) and subsequently transferred to polyacrylamide fluoride (PVDF) membranes (Merck, China). The PVDF membranes were then blocked using 10 % skimmed milk powder in TBST (TBS with 0.1 % Tween) for 2 h. The primary antibodies used in this study were DSPP and DMP1 (Affinity, China), which were applied at a dilution of 1:3000. GAPDH (1:5000, Affinity, China) was utilized as the internal reference. Immune complexes were detected using an anti-rabbit secondary antibody (Abcam, USA). The membranes were washed with TBST four times for 10 min each, followed by incubation with anti-rabbit secondary antibodies for 2 h at room temperature. The Immunoreactive bands were then visualized using a chemiluminescence reagent (Merck Millipore, Darmstadt, Germany) and an imaging system (LAS4000 M). Densitometry analysis was performed using ImageJ software to quantify the observed bands.

2.11. In vivo direct pulp-capping model in rat

Several studies have indicated that pulpitis can be caused not only by bacterial stimulation, but also by physical stimulation or the direct application of pulp capping material to cover the affected pulp [43]. The animal experiments conducted in this study were granted approval by the Animal Ethics Committee of Nanjing University and were conducted in accordance with the guidelines outlined in the National Institutes of Health Guide for the Care and Use of Laboratory Animals. A total of 24 Sprague-Dawley rats, approximately 250 g in weight and aged between 7 and 8 weeks, were randomly assigned to six groups, with each group consisting of four rats: Control group, iRoot BP Plus group (manufactured by Innovative Bioceramics, CA, USA), Hydrogel group, CNPs/Hydrogel group, DMP1/Hydrogel group, and CNPs/DMP1/Hydrogel

Table 1
Primers for RT-qPCR.

Gene	Forward primer sequence	Reverse primer sequence
IL-1 β	TTCGACACATGGGATAACGAGG	TTTTTGCTGTGAGTCCCGGAG
IL-6	TGGGAAGGTTACATCAGATC	GGGTTGGTCCATGTCAATTT
IL-8	CTTCTCCACAACCCTCTG	ACTCCAACCTTTCCACC
ALP	AGCGACACGGACAAGAAGC	GGCAAAGACCGCCACATC
OCN	GAGGGCAGTAAGGTGGTGAA	CGTCTGGAAGCCAATGTG
RUNX2	GCCGTAGAGCAGGGAAGAC	CTGGCTTGGATTAGGGAGTCAC
DMP1	CTCCGAGTTGGACGATGAGG	TCATGCCTGCACTGTTTCATTC
DSPP	GAAGACTGTTATCCTTACG	GTGATCCCCTTTAGATTCTTCC
BSP	AATCTGTGCCACTCACTGC	CAGTCTTCATTTGGTGATTGC
GAPDH	ACTGGGCTTCCACCACCAT	AAGGCCATGCCAGTGAGCTT

group. Following administration of pentobarbital sodium anesthesia, the rats were securely positioned on the operating table.

The bilateral maxillary first molar underwent treatment using a 75 % ethanol solution. The central fossae of the maxillary first molar were then drilled using a 0.08-mm-diameter round bur (Wave dental, China) to expose the pulp. The pulp was subsequently washed with saline to remove any dentin debris. Successful pulp penetration was indicated by the presence of blood leakage. Drugs were administered into the cavity using syringes, with different hydrogel precursors aspirated into 1 mL syringes. A volume of 10 μ L was injected into each selected tooth. Currently, the clinic's commonly used iRoot BP Plus as pulp capping agents. So that iRoot BP Plus was employed for pulp capping in the positive control group, followed by restoration of the occlusal cavities using glass ionomer cement (Fuji IX GP, GC Corporation, Japan). Conversely, in the control group, the pulp was left devoid of any pulp capping agent (Fig. S5). Subsequently, after a duration of 4 weeks, the maxilla and major organs of the animals were collected for further analysis.

2.12. Histological evaluation

The maxilla of the animal, along with its major organs, were immersed in a 10 % neutral buffered formalin solution for a duration of 48 h. Subsequently, a series of standard procedures, encompassing decalcification, dehydration, embedding, and sectioning, were

conducted. The Hematoxylin and eosin (H&E) and the Masson's trichrome staining were used to evaluate the histological changes in the pulp tissue of 4weeks, Immunohistochemistry (IHC) staining to detect the levels of dentinogenic gene (DSPP, 1:200 dilution; DMP1, 1:200 dilution; Affinity) expression. Histopathology images of the heart, liver, spleen, lung, and kidney were employed to assess the toxicity of various hydrogels. The 3DHISTECH slice scanner was utilized to scan all tissue sections, which were then captured using the CaseViewer software.

2.13. Statistical analysis

Statistical analysis was conducted by GraphPad Prism 8 using the one-way analysis of variance. Data were expressed as the mean \pm standard deviation (SD). $P < 0.05$ was considered statistically significant. At least three duplicate samples were tested in all experiments.

3. Results and discussion

3.1. Synthesis and characterization of CNP and CNPs/DMP1/Hydrogel

Chronopoulou et al. [44] successfully encapsulated dexamethasone in PLGA-based nanoparticles and incorporated these nanoparticles into Fmoc-phe3 hydrogel. The controlled and sustained release of dexamethasone was achieved in this nanopolymer/hydrogel system. In a similar vein, Lin et al. [45] developed a photopolymerised

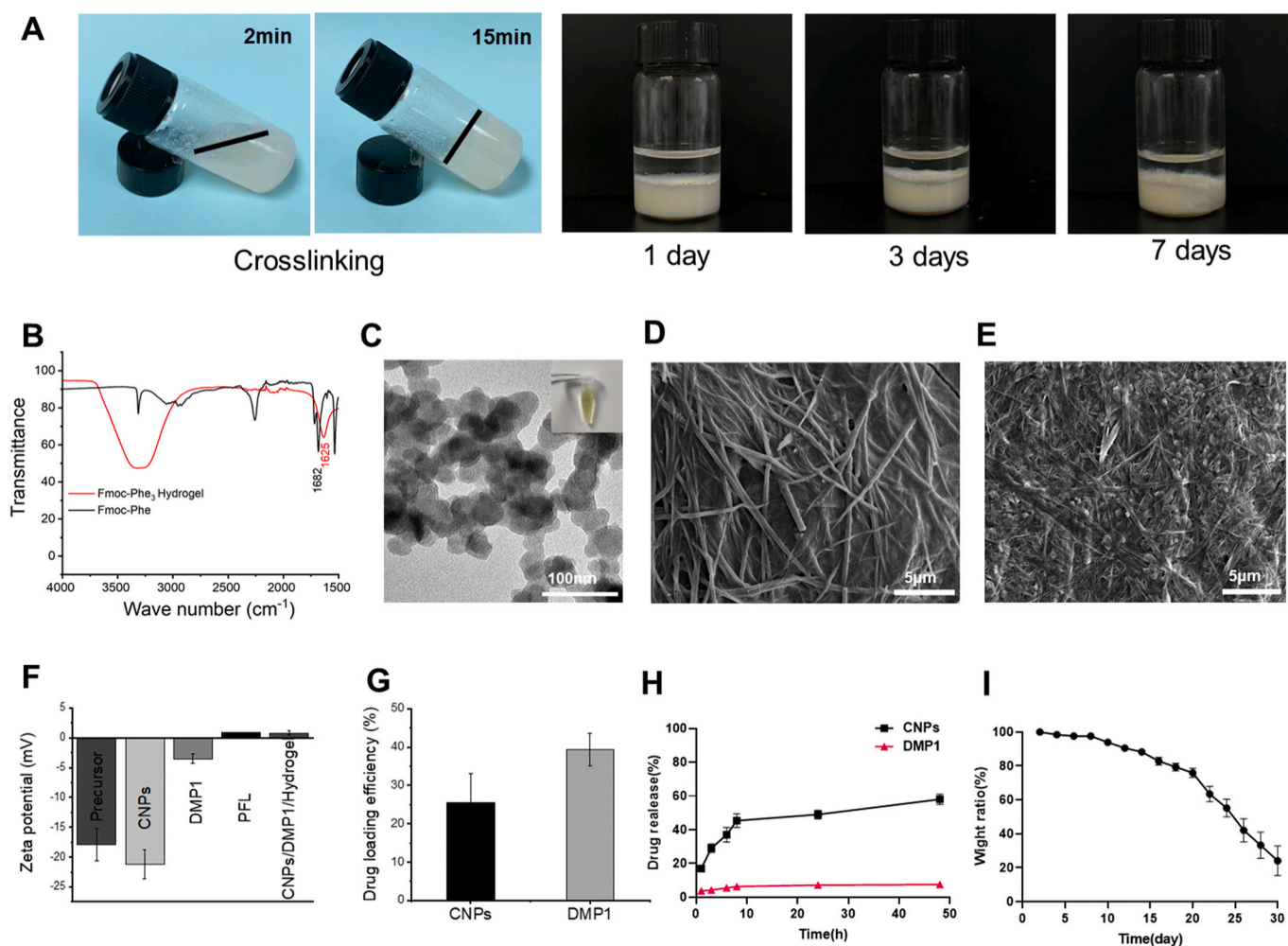


Fig. 1. Synthesis and characterization of CNPs and CNPs/DMP1/Hydrogel. (A) The preparation process and digital photo of CNPs/DMP1/Hydrogel. (B) FTIR spectra of Fmoc-phe₃ Hydrogel and Fmoc-phe. (C) TEM image and digital photos of CNPs. (D) TEM image of Fmoc-phe₃ Hydrogel. (E) TEM image of CNPs/DMP1/Hydrogel. (F) Zeta potential. (G) Drug loading efficiency. (H) The release test of DMP1 and CNPs. (I) The weight change of CNPs/DMP1/Hydrogel.

DMP1/MCF/gel hybrid system, which demonstrated enhanced bone regeneration. Motivated by these achievements, we aimed to load both CNPs and DMP1 into an injectable Fmoc-phe3 hydrogel with exceptional physicochemical properties. This approach allows for injection and adaptation to the anatomical morphology of the dentition, facilitating long-term retention of CNPs and DMP1 in the dental cavity.

The injectable Fmoc-phe2 and phe2 solutions were self-assembled and solidified upon the action of the PFL. The 1, 3 and 7 days digital pictures of CNPs/DMP1/Hydrogel showed its degradation process (Fig. 1A). With the extension of time, the surface of hydrogel in contact with PBS becomes fuzzy, irregular and smaller in volume, and finally degrades and disappears.

In the FTIR spectrum (Fig. 1B), the observed peaks at 1682 cm^{-1} and 3300 cm^{-1} can be attributed to the C=O and -NH- functional groups, respectively. Upon the self-assembly of Fmoc-phe and phe2, a decrease in the stretching vibration intensity of the C=O group was observed. Additionally, the appearance of C=O peaks at 1625 cm^{-1} in Fmoc-phe3 suggests the involvement of two C=O groups in the formation of intermolecular hydrogen bonds. The transition from multiple peaks to a single peak in the vicinity of 1680 cm^{-1} further supports this interaction. Furthermore, the absence of the N-H bending vibration peak at 1500 cm^{-1} indicates the occurrence of polypeptide β folding during the self-assembly process of Fmoc-phe3 hydrogel. The aforementioned findings provide evidence for the successful synthesis of Fmoc-phe3 hydrogel.

The aqueous solution containing the prepared CNPs exhibited an orange coloration, with the CNPs being uniformly dispersed (Fig. 1C). Additionally, the average size of the CNPs was approximately 30 nm. Given that oxidative stress can impact the functionality of dental pulp stem cells, we conducted an investigation into the SOD-mimicking activity of CNPs. Various concentrations of CNPs were assessed using a SOD Assay Kit. The outcomes demonstrated a dose-dependent SOD-like catalytic activity of CNPs, with the elimination percentage of $\cdot\text{O}^{\cdot 2}$ reaching nearly 80 % at a concentration of 120 $\mu\text{g}/\text{mL}$ (Fig. S1).

Fig. 1D and E displays scanning electron microscope (SEM) images of Fmoc-phe3 hydrogels, both with and without the inclusion of CNPs and DMP1. Notably, the presence of black particles within the CNPs/DMP1/Hydrogel complex confirms the successful loading of CNPs. The findings of the study indicate that the surface properties of the negatively charged material exhibit superior suitability for osteoblast attachment and proliferation, surpassing those of the neutral or positively charged materials [46].

Prior to the introduction of PFL, the CNPs/DMP1/Hydrogel components exhibited negative zeta potential values (Fmoc-phe: -15.5 mV, phe2 = -20.9 mV). However, following catalytic treatment with PFL, the zeta potential value shifted to a positive value (CNPs/DMP1/Hydrogel = $+0.819$ mV) (Fig. 1F). This alteration in zeta potential could enhance the uptake efficiency of the loaded drug by facilitating attraction between the negatively charged hDPSCs and CNPs/DMP1/Hydrogel.

The loading percentages of CNPs and DMP1 by Fmoc-phe3 Hydrogel were determined to be 25.6 ± 7.59 % and 39.3 ± 4.28 %, respectively (Fig. 1G).

Subsequently, an investigation was conducted on the drug release behavior of CNPs/DMP1/Hydrogel (Fig. 1H). The release of DMP1 from CNPs/DMP1/Hydrogel occurred gradually over the duration of the experiment, while the release of CNPs initially occurred rapidly and then reached a plateau. CNPs exhibited an initial burst release within the first 8 h, resulting in approximately 45.33 ± 4.16 % of the DMP1 being released from CNPs/DMP1/Hydrogel. Notably, CNPs/DMP1/Hydrogel demonstrated a controlled release of CNPs, with DMP1 being released slowly over a period of 48 h, effectively prolonging its therapeutic effect. The hydrogel exhibited a considerable capacity to facilitate long-term dentin regeneration due to this characteristic.

Following a 30-day immersion period, the residual quantity of CNPs/DMP1/Hydrogel was observed to be 10 % (Fig. 1I), suggesting that the

degradation cycle of the hydrogel may align with the natural cycle of dentin regeneration within living organisms [16].

3.2. Cytotoxicity and cellular uptake

We treated the cells with LPS and hydrogel samples with different drug-loading concentrations. According to the results of the CCK-8 assay, 10 $\mu\text{g}/\text{mL}$ LPS (Fig. S2) and all of the hydrogel samples showed good cytocompatibility (Fig. 2A), however, our results showed that CNPs/DMP1/Hydrogel does not promote cell proliferation, which was inconsistent with previously reported data [47], it may be ascribed to the precise control of PH value during the synthesizing process of the hydrogel. In order to assess the levels of LDH release, as depicted in Fig. 2B, the LDH release rates were found to be less than 5 % [48]. Although the composite material group exhibited slightly higher toxicity compared to the control group, no statistically significant difference was observed between the two. Which means that CNPs/DMP1/Hydrogel exhibited good biocompatibility and did not damage the cell membrane or mitochondrial function. As shown in Fig. 2C, there was no statistical significance in the hemolysis rate after co-incubation of CNPs/DMP1/Hydrogel and red blood solution for 24 h. The viability and proliferation of hDPSCs growing on CNPs/DMP1/Hydrogel were evaluated using Live/Dead staining. As shown in Fig. 2D and E, similar numbers of live cells (green fluorescence) were cultured on control group and CNPs/DMP1/Hydrogel, and few dead cells were seen (red fluorescence). Those results indicated that CNPs/DMP1/Hydrogel was not cytotoxic *in vitro*. In addition, cellular uptake is an important process in biomedical applications of nanomaterials. TEM was employed to evaluate the cellular uptake and detect the intracellular localization of CNPs directly. Cellular uptake is a basic and important process in potential biomedical applications of nanomaterials, TEM images of cells incubated with CNPs/DMP1/Hydrogel for 24 h (Fig. 2F) showed that endosomal compartments containing nanoparticles were seen inside the hDPSCs, indicated CNPs to be taken up by hDPSCs, which was similar to previously reported literature that CNPs widely distributed within the cytoplasm can significantly reduce intracellular ROS, rather than reacting only with ROS produced and released by the cells. All the above results indicate the safety of CNPs/DMP1/Hydrogel in the potential biomedical application.

3.3. CNPs/DMP1/hydrogel reduced inflammatory levels of hDPSCs in the setting of LPS stimulation

There is research evidence that LPS causes an increase in ROS levels within stem cells, high intracellular ROS levels can inhibit the differentiation ability of hDPSCs and even lead to apoptosis of cells [49,50]. The transcription factor NF- κ B is crucial in inflammatory response [51], The activation of the TLR4/MyD88/NF- κ B pathway by LPS leads to the up-regulation of NLRP3 and the expression of pro-IL-1 β genes. Subsequently, the production of ROS stimulated by adenosine triphosphate (ATP) serves as the second signal for NLRP3 activation [52]. In the recent work, the anti-inflammation activity of CNPs/DMP1/Hydrogel was confirmed by fluorescence images of ROS formation in hDPSCs and real-time quantitative PCR. To assess the effect of CNPs/DMP1/Hydrogel on the reduced intracellular ROS, we stimulated hDPSCs by LPS to simulate an inflammatory environment. The qPCR analysis was used to detect the mRNA expression of IL-1 β , IL-6, and IL-8. As shown in Fig. 3A–C, stimulation with 10 $\mu\text{g}/\text{mL}$ LPS increased mRNA expression of IL-1 β , IL-6, and IL-8 compared to a control group. When CNPs/DMP1/Hydrogel and CNPs/Hydrogel were applied to the culture environment, the inflammation-related gene expression of all three groups was reduced, demonstrating that CNPs play a role in mitigating the inflammatory reaction [32]. As shown in Fig. 3D, the ROS level increased in the setting of 10 $\mu\text{g}/\text{mL}$ LPS stimulation. The green fluorescence indicated that ROS levels dramatically declined once cells were treated with CNPs/DMP1/Hydrogel and CNPs/Hydrogel in all groups of

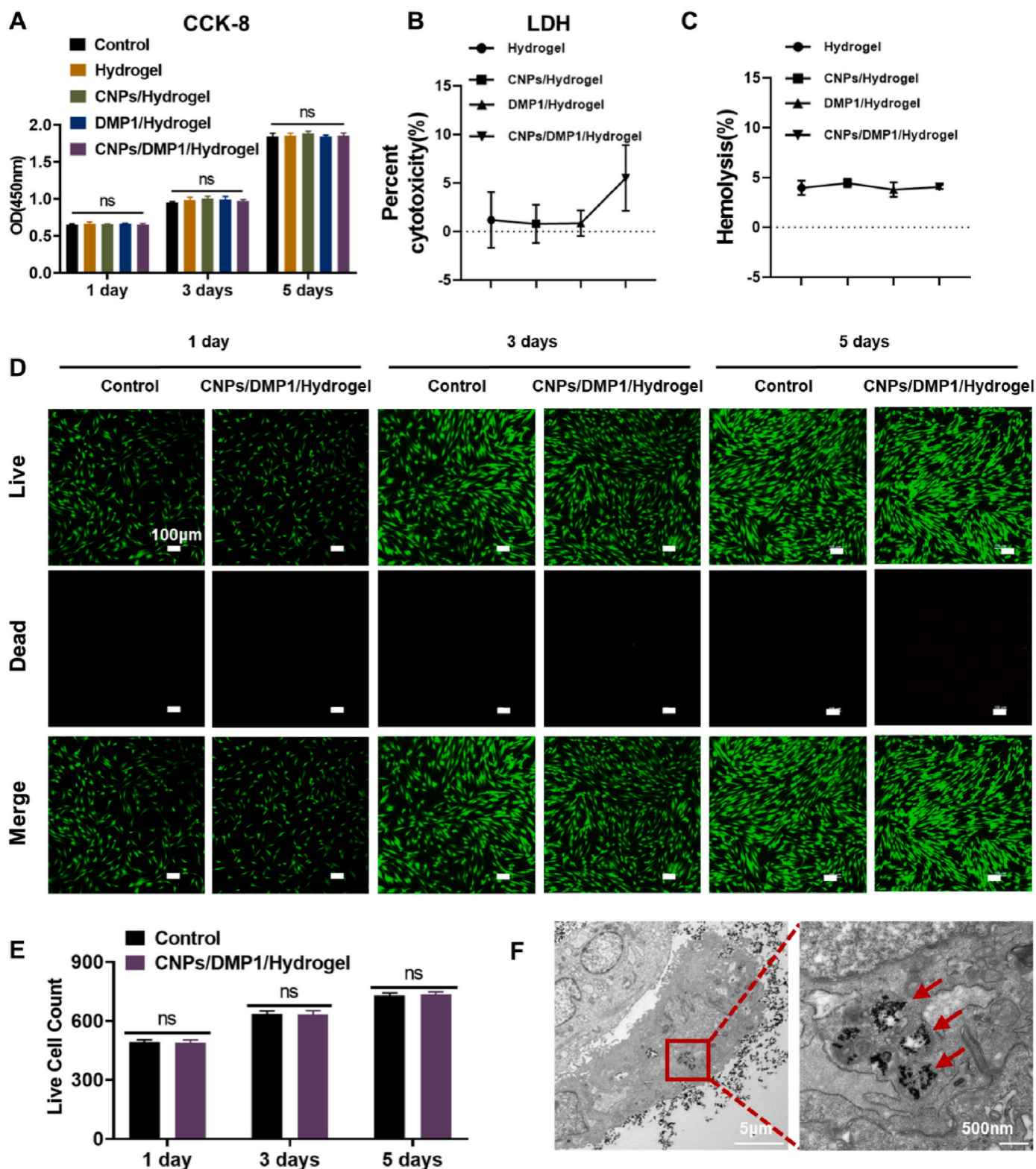


Fig. 2. Cytotoxicity and cellular uptake (A) hDPSCs cultivated on the hydrogels after 1, 3 and 5 days by CCK-8 quantitative analysis. (B) Percent cytotoxicity. (C) Hemolysis with inset photos of different samples. (D) Representative Live/Dead cells fluorescence images of hDPSCs encapsulated in the CNPs/DMP1/Hydrogel after 1,3,5 day of culture (live cells: green; dead cells: red). (E) Viable cell count obtained from the Live/Dead staining assay. (F) hDPSCs treated with CNPs/DMP1/Hydrogel for 24 h (red arrows: CNPs). (All data are expressed as the mean \pm SD. $**P < 0.01$ vs. control group, $***P < 0.001$ vs. control group, $\#P < 0.05$ vs. LPS group, $\#\#P < 0.01$ vs. LPS group, ns: no significant.)

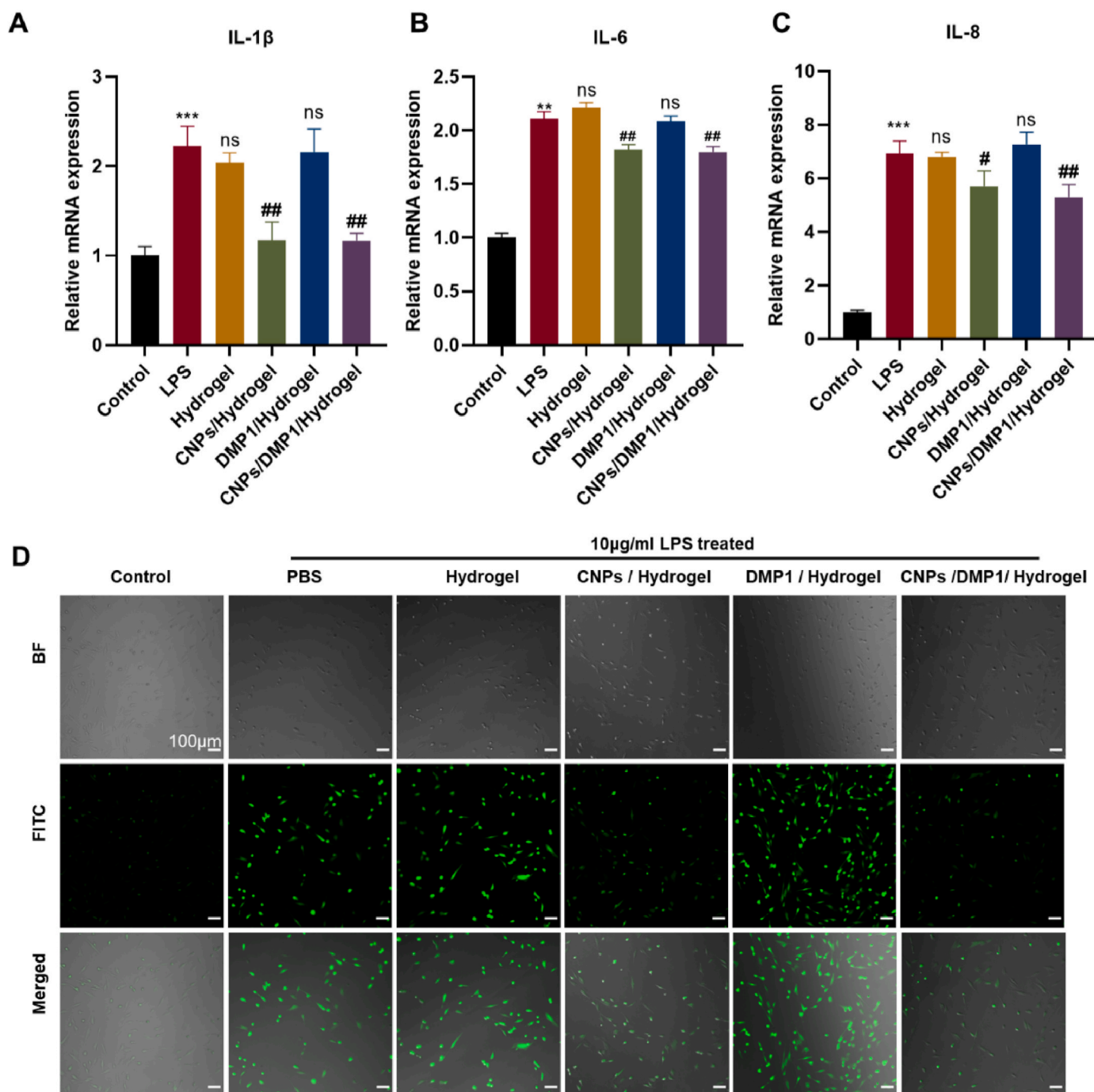


Fig. 3. The anti-inflammation ability treated with CNPs/DMP1/Hydrogel. (A–C) hDPSCs were co-cultured with 10 μ g/mL LPS and different groups for 7 days. CNPs/Hydrogel and CNPs/DMP1/Hydrogel inhibit the expression of inflammatory markers (IL-1 β , IL-6 and IL-8) as detected by qRT-PCR. (D) ROS levels were observed by laser scanning confocal microscopy in hDPSCs treated with 10 μ g/mL LPS alone or combined with different Hydrogel samples. (All data are expressed as the mean \pm SD. ** P < 0.01 vs. control group, *** P < 0.001 vs. control group, # P < 0.05 vs. LPS group, ## P < 0.01 vs. LPS group, ns: no significant.).

LPS treated. The confocal imaging clearly revealed that their reduction can reduce ROS levels at the cellular level rather than only eliminate ROS levels around cells.

3.4. CNPs/DMP1/hydrogel promoted the osteogenic/dentinogenic differentiation of hDPSCs under inflammatory environment

Furthermore, we have elucidated the involvement of CNPs in the modulation of the inflammatory response. It is noteworthy that CNPs not only exert a pivotal role in regulating the inflammatory response of hDPSCs, but also possess the potential to induce dentin formation. Based

on this, we propose the hypothesis that the combination of CNPs, DMP1, and Hydrogel could create a conducive milieu for the anti-inflammatory and odontogenic processes, thereby facilitating efficient dentin regeneration in LPS-induced inflammatory hDPSCs.

We investigated whether the CNPs/DMP1/Hydrogel has a positive effect on the osteogenic/dentinogenic differentiation of hDPSCs under an inflammatory environment. The effect of differentiation was evaluated by ALP activity and staining, Alizarin red S staining and quantification of the mineralized nodules, RT-PCR, and Western Blot. First, hPDLSCs were cultured with different Hydrogel samples or PBS in the presence of 10 μ g/mL LPS for 7 d, 14 d, and 21 d.

Compared with the control group, the ALP activity in the LPS group was significantly reduced on 7 d and 14 d (Fig. 4A and B, Fig. S4B); the Hydrogel group did not significantly affect the amount of mineralized nodules compared with the LPS group. Interestingly, CNPs/DMP1/Hydrogel reversed the inhibitory effect of a high concentration of LPS on ALP activity. The Alizarin red S staining (Fig. 4C, Fig. S4A) and quantification of the mineralized nodules (Fig. 4D, Fig. S4C) showed consistent results.

As shown in Fig. 4E–J, the expression levels of osteogenic/dentinogenic related genes indicated that when hDPSCs were exposed to LPS, the capacity for osteogenic/dentinogenic differentiation was significantly suppressed, which showed the same trend as the ALP activity and Alizarin red S staining.

The gene expressions of dentinogenic-related protein expression levels and the semi-quantitation of DMP1 and DSPP for a duration of 7 days were also assessed (Fig. 4K–L). These findings consistently demonstrated that the dentinogenic markers of hDPSCs were up-regulated at CNPs/DMP1/Hydrogel compared to the LPS groups. These results suggest that CNPs/DMP1/Hydrogel have a positive impact on the osteogenic/dentinogenic differentiation of hDPSCs in an inflammatory environment. However, it is important to note that these simplified models do not account for the interactions between different cell types, as the development of pulpitis is a complex process in vivo [53].

3.5. Therapeutic evaluation in SD rat direct pulp capping models

In order to examine the potential of CNPs/DMP1/Hydrogel in promoting the formation of restorative dentin in vivo, a direct pulp cap model was employed in SD rats. Notably, the Control group exhibited a higher incidence of pulp necrosis compared to the Hydrogel group. The positive control group consisted of iRoot BP Plus, which demonstrated the ability to generate multiple hard tissue formations as evidenced by H&E and Masson staining. However, the observed hard tissues exhibited characteristics of diffuse calcifications rather than authentic reparative dentin. Notably, the CNPs/DMP1/Hydrogel group demonstrated a notable capacity for dentin tissue formation. However, these newly formed mineralized tissues were primarily localized near the CNPs/DMP1/Hydrogel application site, as opposed to widespread pathological calcification throughout the entire root canal system.

After a 4-week period of direct pulp capping in SD rats, both the control and Hydrogel groups exhibited intense inflammatory infiltrate, destruction of the odontoblast layer, and necrotic pulp (Fig. 5A, a, c). Interestingly, there was more necrotic pulp tissue in the control group than in the Hydrogel group, because the Hydrogel had the advantage of insulating the pulp from direct stimulation by glass ions possibly. Indicating that Hydrogel has effective cytoprotective and non-cytotoxic effects and can insulate the pulp from direct stimulation by glass ions. In our in vivo experiments, it was observed that the degradation rate of CNPs/DMP1/Hydrogel correlated with the formation of reparative dentin, and minimal residual hydrogel was evident on H&E sections. Conversely, the interface between pulp tissue and iRoot BP plus exhibited a mild inflammatory response and scattered calcifications. (Fig. 5A and b). Significant inflammation was observed in the DMP1/Hydrogel group, accompanied by frequent deposition of incomplete hard tissue on the dentin walls. Conversely, the CNPs/Hydrogel group exhibited notable improvement in pulp tissue inflammation and a modest promotion of reparative dentin formation. In contrast, the DMP1/CNPs/Hydrogel group exhibited a larger dentin bridge area compared to both the CNPs/Hydrogel group and the iRoot BP Plus group (Fig. 5A, b, d, f). In close proximity to the DMP1/CNPs/Hydrogel group and the CNPs/Hydrogel group, Odontoblast-like cells and newly formed reparative dentin were observed, displaying continuous reparative bridges and distinct dentin tubules. (Fig. 5A, d, f). Further analysis using Masson staining demonstrated that the iRoot BP plus group exhibited numerous diffuse calcifications and non-uniform dyeing. In contrast, the

reparative dentin bridges (RD) in the CNPs/DMP1/Hydrogel group displayed orderly arranged collagen fibers (Fig. 5B, b, f, h, l). Moreover, the region in direct contact with the material exhibited the formation of a continuous dentinal bridge. Afterward, immunohistochemistry analysis of odontogenic marker DSPP and DMP1 in Fig. S6 revealed that DMP1/CNPs/Hydrogel group expressed significantly higher levels of DSPP and DMP1 than the control group.

The biosafety of various composite hydrogel samples was further substantiated through the assessment of tissue sections from vital organs, revealing no substantial variations across groups, thereby affirming its appropriateness for clinical application (Fig. S7). Furthermore, our study was conducted with a limited number of time points, in accordance with previous literature [47], we selected 4 weeks for extraction. However, studies have shown that on the 7 d after capping [42], more continuous dentin regeneration was observed in a 12 weeks study [54]. Longer experimental days should be selected for further experiments so that the final effect of dentin formation and the metabolism of CNPs can be observed. However, it is imperative to synthesize and optimize or chemically modify CNPs [55], a promising nanometer biomaterial, in order to investigate the enhanced odontogenic effects of CNPs with varying sizes. This research aims to ascertain whether CNPs can effectively substitute DMP1, thereby reducing financial expenses and enhancing the clinical applicability of nanomaterials as capping agents in the future. Although CNPs have been shown to reduce oxidative stress levels of periodontal stem cells via the NF- κ B pathway, more work is needed to explore how CNPs inhibit inflammation levels of hDPSCs in the future. Another limitation of this work is that the long-term metabolism of CNPs is unknown. In the context of in vivo experiments, the concentration of CNPs within pulp tissues was predominantly observed in close proximity to the capping agent, which can be ascribed to the constrained nature of the root canal system. The potential capacity of CNPs to traverse the narrow apical foramen and enter the metabolic pathway in vivo, along with their potential to elicit cytotoxic effects due to prolonged presence, necessitates further inquiry into the tissue metabolism of these CNPs. The biodistribution of cerium is commonly assessed using inductively coupled plasma mass spectrometry (ICP-MS). However, our laboratory lacks the necessary equipment to conduct such measurements. Consequently, the ultimate distribution and metabolism of cerium oxide in dental pulp stem cells remain unexplored. Our findings indicate that cerium oxide does not induce harm to vital organs within a 30-day timeframe. If feasible, we intend to extend the duration of the experiment to investigate the toxicity and metabolism of cerium oxide further [56,57]. In conclusion, the results of our study indicate that the utilization of DMP1/CNPs/Hydrogel exhibits significant efficacy in mitigating symptoms of pulpitis and facilitating the formation of reparative dentin during direct pulp capping procedures in SD rats. These findings serve as a crucial foundation for the future development of optimal materials for pulp capping applications.

4. Conclusions

In conclusion, the synthesis of CNPs/DMP1/Hydrogel was undertaken and its physicochemical properties and biocompatibility were examined. The impact of CNPs on the behavior and function of hDPSCs in inflammatory states was demonstrated, highlighting its novelty. In vitro experiments revealed that CNPs/DMP1/Hydrogel facilitated osteogenic/dentinogenic differentiation of hDPSCs, while in vivo studies showed accelerated dentin regeneration and preservation of pulp necrosis outcomes. It is our belief that CNPs/DMP1/Hydrogel, as a dental pulp capping biomaterial, offers a novel, safe, and cost-effective solution for sustained in situ drug delivery, with promising prospects for future clinical applications.

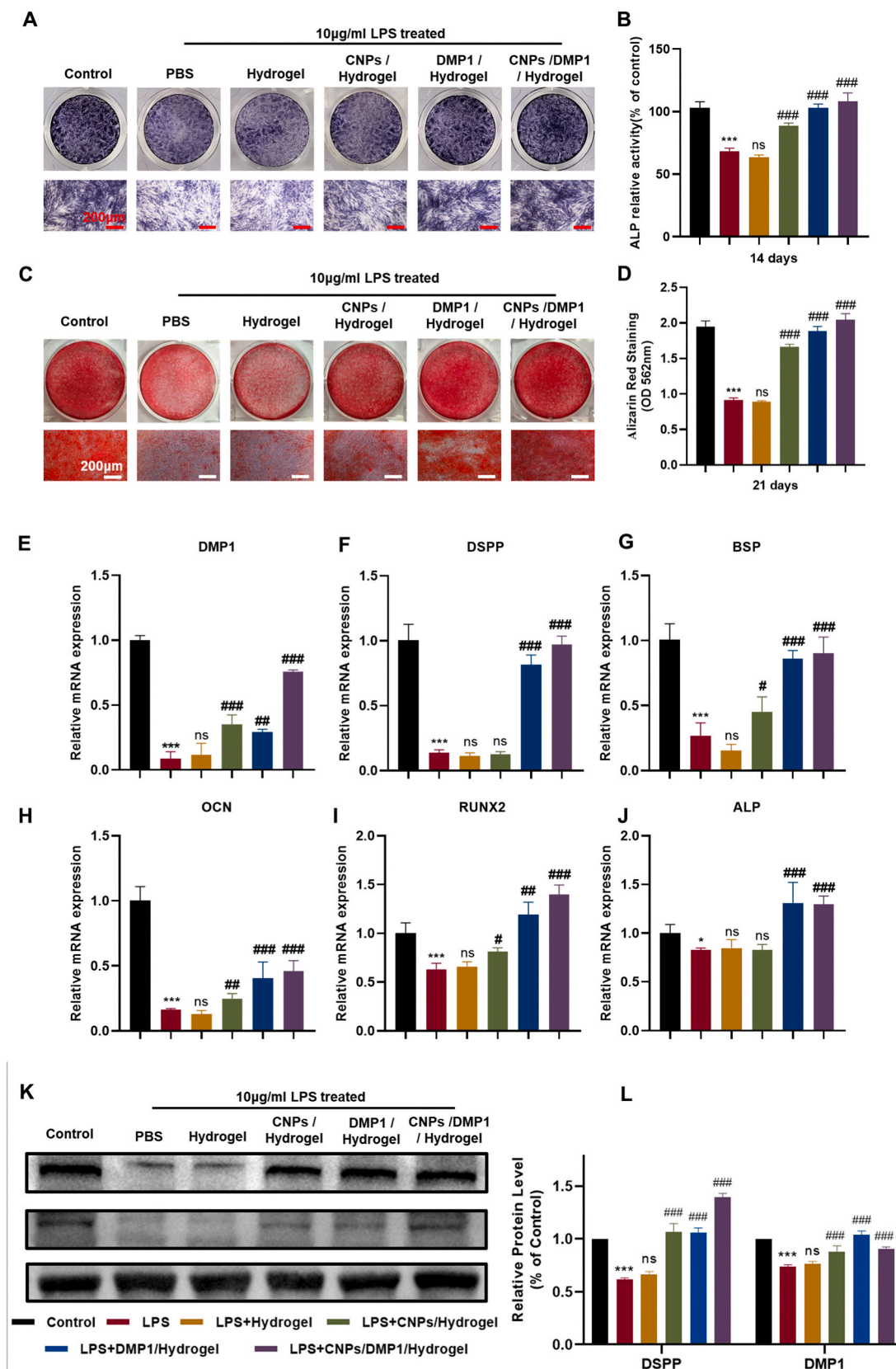


Fig. 4. Osteogenic/dentinogenic effects of CNPs/DMP1/Hydrogel on hPSCs in the setting of LPS stimulation. (A) ALP stained images on 7 d. (B) ALP relative activity on 14 d. (C-D) ARS stained images and the OD values at 562 nm at 21 d. (E-J) Osteogenic/dentinogenic related gene expressions on 7 d. (K) Dentinogenic-related protein expressions on 7 d. (L) The semi-quantitation of the expression of DSPP and DMP1 on 7 d. (* $P < 0.05$ vs. control group, *** $P < 0.001$ vs. control group, # $P < 0.05$ vs. LPS group, ## $P < 0.01$ vs. LPS group, ### $P < 0.01$ vs. LPS group, ns: no significant.).

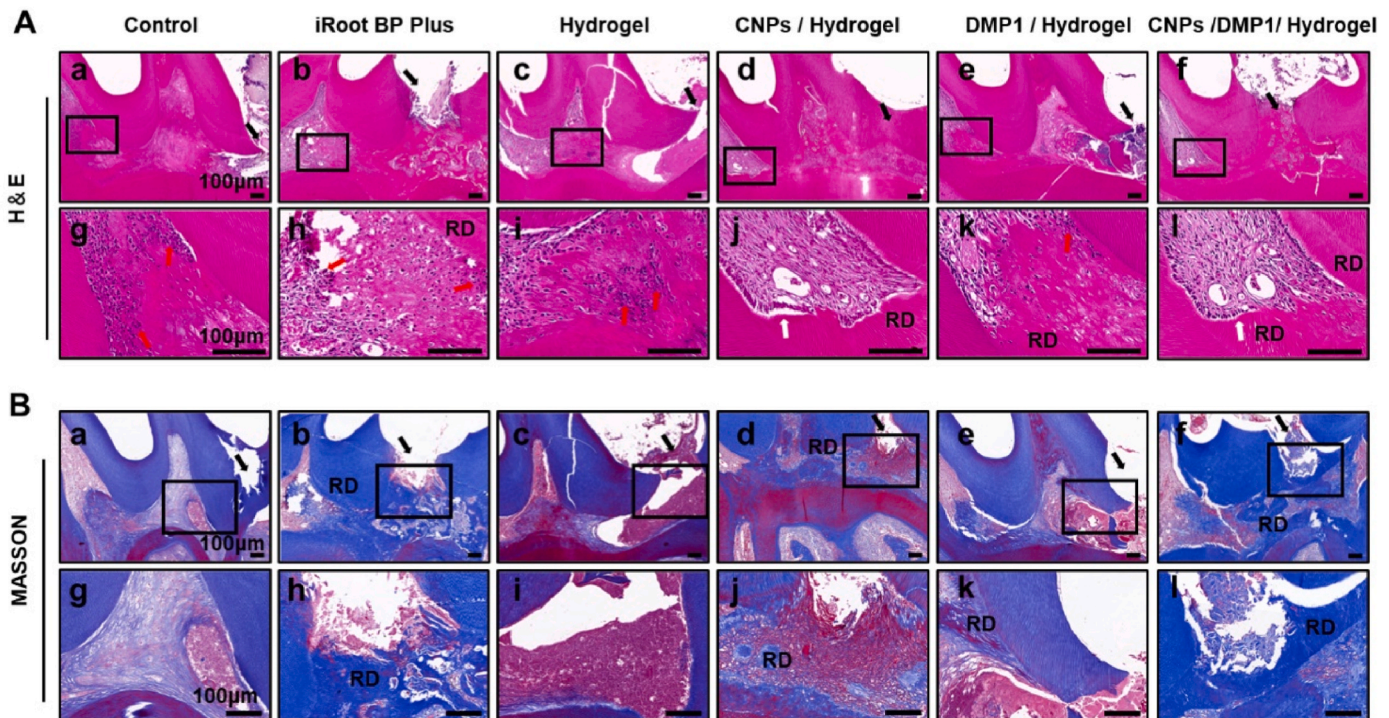


Fig. 5. CNPs/DMP1/Hydrogel exhibits a good promotion of dentin formation in vivo direct pulp-capping model in rats. (A) Representative images of H&E staining of the pulp tissue around maxillary first molars after 4 weeks of treatment. (RD: reparative dentin, red arrow: inflammatory cell, blank arrow: odontoblast-like cell and newly formed dentinal tubules, black arrow: the exposure site), (B) Representative images of Masson staining of the pulp tissue in the first molars. (RD: reparative dentin, black arrow: the exposure site)

CRediT authorship contribution statement

Yue Zhao: Conceptualization, Investigation, Methodology, Writing - original draft, Writing - review & editing. **Lutong Song:** Data curation, Investigation, Software. **Mengchen Li:** Data curation, Methodology, Software. **Haoran Peng:** Data curation, Formal analysis. **Xinyi Qiu:** Formal analysis, Methodology. **Yuyang Li:** Investigation, Software. **Bijun Zhu:** Investigation, Visualization. **Chao Liu:** Funding acquisition, Writing - review & editing. **Shuangshuang Ren:** Funding acquisition, Methodology, Project administration, Resources, Validation, Writing - review & editing. **Leiyang Miao:** Conceptualization, Funding acquisition, Project administration, Resources, Supervision, Validation, Writing - review & editing.

Declaration of competing interest

The authors declare that they have no known competing financial interests or personal relationships that could have appeared to influence the work reported in this paper.

Data availability

Data will be made available on request.

Acknowledgements

This study was supported by “2015” Cultivation Program for Reserve Talents for Academic Leaders of Nanjing Stomatological School, Medical School of Nanjing University (number 0223A203); “2015” Cultivation Program for Reserve Talents for Academic Leaders of Nanjing Stomatological School, Medical School of Nanjing University (number 0223A210); the National Natural Science Foundation of China (number 82001049); Nanjing Clinical Research Center for Oral Diseases (number 2019060009); Natural Science Foundation of Jiangsu under Grant

(number BK20221177); and the Natural Science Foundation of Jiangsu Province under Grant (number BK20200665).

Appendix A. Supplementary data

Supplementary data to this article can be found online at <https://doi.org/10.1016/j.mtbio.2023.100907>.

References

- [1] M.A. Saghiri, A. Asatourian, F. Garcia-Godoy, N. Sheibani, Effect of biomaterials on angiogenesis during vital pulp therapy, *Dent. Mater. J.* 35 (5) (2016) 701–709.
- [2] G. Mikrogeorgis, E. Eirinaki, V. Kapralos, A. Koutroulis, K. Lyroudia, I. Pitas, Diagnosis of vertical root fractures in endodontically treated teeth utilising Digital Subtraction Radiography: a case series report, *Aust. Endod. J.* 44 (3) (2018) 286–291.
- [3] J. Ghoddsi, M. Forghani, I. Parisay, New approaches in vital pulp therapy in permanent teeth, *Iran. Endod. J.* 9 (1) (2014) 15–22.
- [4] L. Bjørndal, S. Simon, P.L. Tomson, H.F. Duncan, Management of deep caries and the exposed pulp, *Int. Endod. J.* 52 (7) (2019) 949–973.
- [5] B. Bagis, P. Atilla, N. Cakar, U. Hasanreisoglu, Immunohistochemical evaluation of endothelial cell adhesion molecules in human dental pulp: effects of tooth preparation and adhesive application, *Arch. Oral Biol.* 52 (8) (2007) 705–711.
- [6] P.R. Cooper, M.J. Holder, A.J. Smith, Inflammation and regeneration in the dentin-pulp complex: a double-edged sword, *J. Endod.* 40 (4 Suppl) (2014) S46–S51.
- [7] S.H. Lee, C.H. Kim, J.Y. Yoon, E.J. Choi, M.K. Kim, J.U. Yoon, H.Y. Kim, E.J. Kim, Lidocaine intensifies the anti-osteogenic effect on inflammation-induced human dental pulp stem cells via mitogen-activated protein kinase inhibition, *J. Dent. Sci.* 18 (3) (2023) 1062–1072.
- [8] C. Bucchi, A. Bucchi, P. Martínez-Rodríguez, Biological properties of dental pulp stem cells isolated from inflamed and healthy pulp and cultured in an inflammatory microenvironment, *J. Endod.* 49 (4) (2023) 395–401 e6.
- [9] C.C. Winterbourn, Reconciling the chemistry and biology of reactive oxygen species, *Nat. Chem. Biol.* 4 (5) (2008) 278–286.
- [10] T. Giraud, C. Jeanneau, C. Rombouts, H. Bakhtiar, P. Laurent, I. About, Pulp capping materials modulate the balance between inflammation and regeneration, *Dent. Mater.* 35 (1) (2019) 24–35.
- [11] C. Liang, L. Liao, W. Tian, Stem cell-based dental pulp regeneration: insights from signaling pathways, *Stem Cell Rev Rep* 17 (4) (2021) 1251–1263.
- [12] W. Zhang, P.C. Yelick, Vital pulp therapy-current progress of dental pulp regeneration and revascularization, *Int J Dent* 2010 (2010), 856087.

- [13] Z. Siddiqui, A.M. Acevedo-Jake, A. Griffith, N. Kadinceme, K. Dabek, D. Hindi, K. K. Kim, Y. Kobayashi, E. Shimizu, V. Kumar, Cells and material-based strategies for regenerative endodontics, *Bioact. Mater.* 14 (2022) 234–249.
- [14] J. Camilleri, Investigation of Biodentine as dentine replacement material, *J. Dent.* 41 (7) (2013) 600–610.
- [15] T. Komabayashi, Q. Zhu, R. Eberhart, Y. Imai, Current status of direct pulp-capping materials for permanent teeth, *Dent. Mater.* J. 35 (1) (2016) 1–12.
- [16] E.M. Rodrigues, A.L.G. Cornélio, L.B. Mestieri, A.S.C. Fuentes, L.P. Salles, C. Rossa-Junior, G. Faria, J.M. Guerreiro-Tanomaru, M. Tanomaru-Filho, Human dental pulp cells response to mineral trioxide aggregate (MTA) and MTA Plus: cytotoxicity and gene expression analysis, *Int. Endod. J.* 50 (8) (2017) 780–789.
- [17] N. Akhlaghi, A. Khademi, Outcomes of vital pulp therapy in permanent teeth with different medicaments based on review of the literature, *Dent. Res. J.* 12 (5) (2015) 406–417.
- [18] S. Shi, Z.F. Bao, Y. Liu, D.D. Zhang, X. Chen, L.M. Jiang, M. Zhong, Comparison of in vivo dental pulp responses to capping with iRoot BP Plus and mineral trioxide aggregate, *Int. Endod. J.* 49 (2) (2016) 154–160.
- [19] N. Mahgoub, B. Alqadasi, K. Aldhorae, A. Assiry, Z.M. Altawili, H. Tao, Comparison between iRoot BP plus (EndoSequence root repair material) and mineral trioxide aggregate as pulp-capping agents: a systematic review, *J. Int. Soc. Prev. Community Dent.* 9 (6) (2019) 542–552.
- [20] R. Islam, Y. Toida, F. Chen, T. Tanaka, S. Inoue, T. Kitamura, Y. Yoshida, A. Chowdhury, H.M.A. Ahmed, H. Sano, Histological evaluation of a novel phosphorylated pullulan-based pulp capping material: an in vivo study on rat molars, *Int. Endod. J.* 54 (10) (2021) 1902–1914.
- [21] M. Li, Y. Wang, J. Xue, Q. Xu, Y. Zhang, J. Liu, H. Xu, Z. Guan, C. Bian, G. Zhang, Y. Yu, Baicalin can enhance odonto/osteogenic differentiation of inflammatory dental pulp stem cells by inhibiting the NF- κ B and β -catenin/Wnt signaling pathways, *Mol. Biol. Rep.* 50 (5) (2023) 4435–4446.
- [22] M. Alipour, S. Fadar, M. Aghazadeh, R. Salehi, H. Samadi Kafil, L. Roshangar, E. Mousavi, Z. Aghazadeh, Synthesis, characterization, and evaluation of curcumin-loaded endodontic reparative material, *J. Biochem. Mol. Toxicol.* 35 (9) (2021), e22854.
- [23] Y. Yang, L. Guo, Z. Wang, P. Liu, X. Liu, J. Ding, W. Zhou, Targeted silver nanoparticles for rheumatoid arthritis therapy via macrophage apoptosis and Repolarization, *Biomaterials* 264 (2021), 120390.
- [24] C. Ni, J. Zhou, N. Kong, T. Bian, Y. Zhang, X. Huang, Y. Xiao, W. Yang, F. Yan, Gold nanoparticles modulate the crosstalk between macrophages and periodontal ligament cells for periodontitis treatment, *Biomaterials* 206 (2019) 115–132.
- [25] Y. Sun, X. Sun, X. Li, W. Li, C. Li, Y. Zhou, L. Wang, B. Dong, A versatile nanocomposite based on nanoceria for antibacterial enhancement and protection from aPDT-aggravated inflammation via modulation of macrophage polarization, *Biomaterials* 268 (2021), 120614.
- [26] H. Li, P. Xia, S. Pan, Z. Qi, C. Fu, Z. Yu, W. Kong, Y. Chang, K. Wang, D. Wu, X. Yang, The advances of ceria nanoparticles for biomedical applications in orthopaedics, *Int. J. Nanomed.* 15 (2020) 7199–7214.
- [27] X. Li, M. Qi, X. Sun, M.D. Weir, F.R. Tay, T.W. Oates, B. Dong, Y. Zhou, L. Wang, H. H.K. Xu, Surface treatments on titanium implants via nanostructured ceria for antibacterial and anti-inflammatory capabilities, *Acta Biomater.* 94 (2019) 627–643.
- [28] S. Ren, Y. Zhou, K. Zheng, X. Xu, J. Yang, X. Wang, L. Miao, H. Wei, Y. Xu, Cerium oxide nanoparticles loaded nanofibrous membranes promote bone regeneration for periodontal tissue engineering, *Bioact. Mater.* 7 (2022) 242–253.
- [29] S.K. Jun, J.Y. Yoon, C. Mahapatra, J.H. Park, H.W. Kim, H.R. Kim, J.H. Lee, H. H. Lee, Ceria-incorporated MTA for accelerating odontoblastic differentiation via ROS downregulation, *Dent. Mater.* 35 (9) (2019) 1291–1299.
- [30] C. Mahapatra, R.K. Singh, J.H. Lee, J. Jung, J.K. Hyun, H.W. Kim, Nano-shape varied cerium oxide nanomaterials rescue human dental stem cells from oxidative insult through intracellular or extracellular actions, *Acta Biomater.* 50 (2017) 142–153.
- [31] Y. Yu, S. Zhao, D. Gu, B. Zhu, H. Liu, W. Wu, J. Wu, H. Wei, L. Miao, Cerium oxide nanozyme attenuates periodontal bone destruction by inhibiting the ROS-NF κ B pathway, *Nanoscale* 14 (7) (2022) 2628–2637.
- [32] A. Rangiani, Z.G. Cao, Y. Liu, A. Voisey Rodgers, Y. Jiang, C.L. Qin, J.Q. Feng, Dentin matrix protein 1 and phosphate homeostasis are critical for postnatal pulp, dentin and enamel formation, *Int. J. Oral Sci.* 4 (4) (2012) 189–195.
- [33] R.S. Prescott, R. Alsanea, M.I. Fayad, B.R. Johnson, C.S. Wenckus, J. Hao, A. S. John, A. George, In vivo generation of dental pulp-like tissue by using dental pulp stem cells, a collagen scaffold, and dentin matrix protein 1 after subcutaneous transplantation in mice, *J. Endod.* 34 (4) (2008) 421–426.
- [34] T. Liu, J. Wang, X. Xie, K. Wang, T. Sui, D. Liu, L. Lai, H. Zhao, Z. Li, J.Q. Feng, DMP1 ablation in the rabbit results in mineralization defects and abnormalities in haversian canal/osteon microarchitecture, *J. Bone Miner. Res.* 34 (6) (2019) 1115–1128.
- [35] K. Saito, M. Nakatomi, H. Ohshima, Dentin matrix protein 1 compensates for lack of osteopontin in regulating odontoblastlike cell differentiation after tooth injury in mice, *J. Endod.* 46 (1) (2020) 89–96.
- [36] S. Kongkiatkamon, A. Ramachandran, K.L. Knoernschild, S.D. Campbell, C. Sukotjo, A. George, Dentin matrix protein 1 on titanium surface facilitates osteogenic differentiation of stem cells, *Molecules* 26 (22) (2021).
- [37] L. Wang, H. Fu, W. Wang, Y. Liu, X. Li, J. Yang, L. Li, G. Wu, Y. Pan, Notoginsenoside R1 functionalized gelatin hydrogels to promote reparative dentinogenesis, *Acta Biomater.* 122 (2021) 160–171.
- [38] J. Tavakoli, Y. Tang, Hydrogel based sensors for biomedical applications: an updated review, *Polymers* 9 (8) (2017).
- [39] R. Binaymotlagh, L. Chronopoulou, F.H. Haghighi, I. Fratoddi, C. Palocci, Peptide-based hydrogels: new materials for biosensing and biomedical applications, *Materials* 15 (17) (2022).
- [40] L. Chronopoulou, S. Sennato, F. Bordin, D. Giannella, A. Di Nitto, A. Barbeta, M. Dentini, A.R. Togni, G.I. Togni, S. Moschini, C. Palocci, Designing unconventional Fmoc-peptide-based biomaterials: structure and related properties, *Soft Matter* 10 (12) (2014) 1944–1952.
- [41] Y. Li, H. Peng, W. Tang, D. Gu, S. Ren, Y. Yu, J. Yang, L. Miao, Accelerating periodontal regeneration through injectable hydrogel-enabled sequential delivery of nanoceria and erythropoietin, *Mater. Des.* 225 (2023).
- [42] J. Chen, H. Xu, K. Xia, S. Cheng, Q. Zhang, Resolvin E1 accelerates pulp repair by regulating inflammation and stimulating dentin regeneration in dental pulp stem cells, *Stem Cell Res. Ther.* 12 (1) (2021) 75.
- [43] J. Wu, Q. Wang, Q. Han, H. Zhu, M. Li, Y. Fang, X. Wang, Effects of Nel-like molecule-1 and bone morphogenetic protein 2 combination on rat pulp repair, *J. Mol. Histol.* 50 (3) (2019) 253–261.
- [44] L. Chronopoulou, S. Margheritelli, Y. Toumia, G. Paradossi, F. Bordin, S. Sennato, C. Palocci, Biosynthesis and characterization of cross-linked Fmoc peptide-based hydrogels for drug delivery applications, *Gels* 1 (2) (2015) 179–193.
- [45] S. Lin, L. Cao, Q. Wang, J. Du, D. Jiao, S. Duan, J. Wu, Q. Gan, X. Jiang, Tailored biomimetic hydrogel based on a photopolymerised DMP1/MCF/gelatin hybrid system for calvarial bone regeneration, *J. Mater. Chem. B* 6 (3) (2018) 414–427.
- [46] J.H. Lee, M.S. Kang, C. Mahapatra, H.W. Kim, Effect of aminated mesoporous bioactive glass nanoparticles on the differentiation of dental pulp stem cells, *PLoS One* 11 (3) (2016), e0150727.
- [47] R. Richert, M. Ducret, B. Alliot-Licht, M. Bekhouche, S. Gobert, J.C. Farges, A critical analysis of research methods and experimental models to study pulpitis, *Int. Endod. J.* 55 (Suppl 1) (2022) 14–36.
- [48] M. Broussas, L. Broyer, L. Goetsch, Evaluation of antibody-dependent cell cytotoxicity using lactate dehydrogenase (LDH) measurement, *Methods Mol. Biol.* 988 (2013) 305–317.
- [49] C.L. Bigarella, R. Liang, S. Ghaffari, Stem cells and the impact of ROS signaling, *Development* 141 (22) (2014) 4206–4218.
- [50] C. Llena, M. Collado-González, D. García-Bernal, R.E. Oñate-Sánchez, C. M. Martínez, J.M. Moraleda, F.J. Rodríguez-Lozano, L. Forner, Comparison of diffusion, cytotoxicity and tissue inflammatory reactions of four commercial bleaching products against human dental pulp stem cells, *Sci. Rep.* 9 (1) (2019) 7743.
- [51] G. Bonizzi, M. Karin, The two NF-kappaB activation pathways and their role in innate and adaptive immunity, *Trends Immunol.* 25 (6) (2004) 280–288.
- [52] A. Zhang, P. Wang, X. Ma, X. Yin, J. Li, H. Wang, W. Jiang, Q. Jia, L. Ni, Mechanisms that lead to the regulation of NLRP3 inflammasome expression and activation in human dental pulp fibroblasts, *Mol. Immunol.* 66 (2) (2015) 253–262.
- [53] L. Chronopoulou, S. Lorenzoni, G. Masci, M. Dentini, A.R. Togni, G. Togni, F. Bordin, C. Palocci, Lipase-supported synthesis of peptidic hydrogels, *Soft Matter* 6 (11) (2010).
- [54] D Gu, H Liu, X Qiu, Y Yu, X Tang, C Liu, L Miao, Erythropoietin induces odontoblastic differentiation of human-derived pulp stem cells via EphB4-Mediated MAPK signaling pathway, *Oral Dis* 29 (7) (2023 Oct) 2816–2826.
- [55] H. Olsson, J.R. Davies, K.E. Holst, U. Schröder, K. Petersson, Dental pulp capping: effect of Emdogain Gel on experimentally exposed human pulps, *Int. Endod. J.* 38 (3) (2005) 186–194.
- [56] U.M. Graham, M.T. Tseng, J.B. Jasinski, R.A. Yokel, J.M. Unrine, B.H. Davis, A. K. Dozier, S.S. Hardas, R. Sultana, E.A. Grulke, D.A. Butterfield, In vivo processing of ceria nanoparticles inside liver: impact on free-radical scavenging activity and oxidative stress, *Chempluschem* 79 (8) (2014) 1083–1088.
- [57] B.A. Rzigalinski, C.S. Carfagna, M. Ehrlich, Cerium oxide nanoparticles in neuroprotection and considerations for efficacy and safety, *Wiley Interdiscip Rev Nanomed Nanobiotechnol* 9 (4) (2017).